Development of Field Oriented Control for Induction Motor using TMS320F28069 32-bit Microcontroller

Karchung[1*], Sakda Somkun[2], Somporn Ruangsinchaiwanich[3]

[1]Jigme Namgyel Engineering College, Royal University of Bhutan, Samdrup Jongkhar 41002, Bhutan
[2]School of Renewable Energy and Smart Grid Technology, Naresuan University, Phitsanulok 65000, Thailand
[3]Faculty of Engineering, Naresuan University, Phitsanulok 65000, Thailand
***Corresponding author's email:** karchung1990@gmail.com
Received: 15 October 2021, Revised: 2 March 2022, Accepted: 15 May 2022

Abstract

Induction motors have recently emerged as an intriguing topic in the realm of industrial drives. The various control techniques are used to decrease torque, flux, current, and speed ripple. However, the issue at lower or near-zero reference is still an issue. Moreover, very little literature is there on the development of converters in the laboratory. This paper aims at developing a smart F28069M-based converter in the laboratory to dynamically control the speed of a three-phase induction motor with a modern control algorithm to achieve the best possible performance to have minimized harmonic production, the best utilization of input power, and have the best adaptability to the change in input frequency to suit the general application in the industrial drive. To achieve the set objectives, a converter is adapted on the 3 HP induction motor. The F28069M launchpad is used to program and control the IGBT switches used in converters. The establishment of set objectives is possible with the use of vector control methods with space vector modulation algorithms. The motor's actual speed is compared with the user-defined speed reference and current harmonics and torque ripples are monitored. The results obtained showed satisfaction for all tests being considered. The modeling aspect is achieved in the MATLAB Simulink and script programming. The study is expected to be used in improving the control of electric vehicles and other industrial drives.

Keywords:

Field-Oriented Control, Induction Motor, MATLAB Simulink, Vector Control

1. Introduction

Induction motors are widely used in industry because they are simple, inexpensive, long-lasting, robust, dependable, and require less maintenance. However, DC motors were mostly used in the application where variable speed is required because induction motors are constant speed motors. The market for variable speed drive is increasing in both size and number displacing the traditional fixed supply because the new system has improved efficiency in terms of energy conversion and functionality [1]. Due to the increasing demand for bigger motors in the industries, multilevel inverters are receiving increased attention [2-7]. Although there are tremendous applications of converters, not limited to motor control, renewable energy, and electric vehicle; very limited literature explains the design and development of converters in the laboratory. It is difficult for the researchers to follow on the limited literature that too is quite old. Therefore, this paper will discuss extensively the design aspect of the converter.

Lately, several techniques for controlling the speed of a three-phase induction motor were introduced. The methods include V/F control, direct torque control, and vector (field-oriented) control. For the motor performance on the constant load, the torque should be steady despite transients. To keep the torque steady, a constant flux is required [8]. To mitigate these, the field-oriented control (FOC)

commonly called vector control (VC) is proposed. It is the most recent and efficient speed control technique used for the control of AC machines by employing the variable frequency drive technology [9]. The FOC is also used to overcome the slow response of induction motors and to achieve decoupled flux and torque characteristics [10-12]. Now the understanding of FOC has become easier because the novelty of Parks transform has become renowned in the engineering world [13]. The major drawback of FOC includes rotor time constant sensitivity and erroneous flux estimation at lower speeds. To overcome this, immediate rotor position or field angle is necessary to be implemented [14]. This issue is taken care of by considering the indirect or feed-forward vector control (IFOC). In this method, the drives can operate smoothly in the speed ranges from zero to high-speed field-weakening region. This research thus has adopted this method.

The Direct Torque Control (DTC) is rival for FOC as it can achieve efficient decoupled control of flux and electromagnetic torque [11, 15]. It does not require coordinate transformation or current regulation, and it has a simpler control scheme with faster response and low dependence on the machine parameters compared to FOC. The comparative study on the similarities and differences can be found in the literature [14]. Nowadays, DTC which employs a space vector modulator is gaining popularity because of decreased torque and flux ripples as well as a set switching frequency [16-19]. On the contrary, it produces high flux and torque ripples due to variable switching frequency [20], which makes the FOC still superior.

The presence of harmonics causes a non-sinusoidal response, and heat and torque pulsation within the machine. Therefore, the selection of an effective modulation technique is critical for the FOC of induction motor drives. The different PWM techniques used in the inverter-fed induction motor include Sine PWM (SPWM), space vector modulation (SVM), carrier-based PWM, selective harmonic elimination PWM, and harmonic based PWM. The Sine PWM and SVM are popular and widely used PWM strategies due to the simplicity of the application [6]. When the machine current is regulated, the existence of ripples in this current loop may cause numerous zero-crossing difficulties in the SPWM [10]. However, with eight vector states, SVM, also known as digitized PWM, can be readily implemented with sophisticated microcontrollers during hardware design [10]. Moreover, it provides higher DC-bus utilization, lower switching loss, and reduced harmonic distortion (THD) compared to SPWM [21-22]. It is proposed to replace the switching table with voltage vector selection [15]. If the switching frequency can be preserved at a constant value, then the flux and torque ripples can be reduced to a greater extent. Therefore, the SVM is adopted for this research.

2. Materials and Methods

2.1. System Architecture

The current industry applications (ranging from low to high power) require AC power with changeable amplitude and frequency. Variable AC power is created by converting utility AC power with fixed amplitude and frequency to AC/DC/AC power. Power converters change the frequency and amplitude of an alternating current value to meet the needs of the system. A pulse width modulated voltage source inverter (PWM-VSI) with a front-end diode rectifier and a DC-link capacitor is the most common architecture in today's off-the-shelf AC/DC/AC power converter. The diode rectifier-based SVM-VSI, depicted in Fig. 1, has been designed and assembled in the laboratory. This structure is made up of two phases of power conversion and an intermediate energy storage element. The diode rectifier in the utility converts the fixed AC power to an unregulated DC power. After that, the converted DC power is stored in the DC-link capacitor. Using high-frequency switching, the SVM-VSI then creates an AC waveform with adjustable amplitude and frequency. The detailed hardware architecture is presented in a later section.

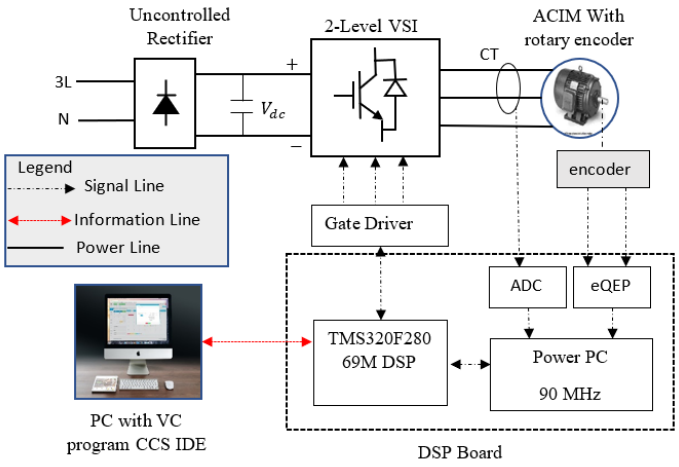

Fig. 1 Motor control architecture with TMS320F28069M.

The stator currents from the motor terminal are measured by CT and are converted to a digital value and are assigned to i_a and i_b variables. The datasheet of the current sensor showed a sensitivity of 80 mV/A. The scaling factor of CT is calculated by illustrating the analog-to-digital converter (ADC). The analog to digital conversion happens in three steps. (a) from the physical measured value from the output of the inverter, (b) CT measures the physical value and sends in range of ±5 V to ADC, and (c) the offset correction and scaling to suit DSP. The scaling factor is calculated by using the relation:

$$K_{scaling}=\frac{3.3}{I_{bc}K_H} \tag{1}$$

Where, I_{bc} is the base current and K_H is the CT sensitivity factor. In this project, the base current value was 7.0710 and the CT sensitivity factor is 0.008 (From datasheet). Therefore, the scaling factor is 5.8336.

The speed encoder measures rotor speed. An incremental encoder disk is patterned with a track of slots along its periphery. These slots create an alternating pattern of dark and light lines. The disk count is defined by the number of dark and light line pairs that occur per revolution (lines per revolution). Therefore, every rotary encoder is defined by its pulse per revolution/lines per revolution (PPR). Index signal or zero references is added to generate a signal that occurs once per revolution, which can be used to indicate an absolute position. Once the settings and definition are completed, the rotor is calculated using the formula:

$$v(k)=\frac{x(k)-x(k-1)}{T}=\frac{\Delta X}{T} \tag{2}$$

Where $v(k)$ and $x(k)$ are velocities, and position at instant k, $x(k-1)$ is position at instant $k-1$, and T is fixed unit time or inverse of velocity calculation rate, and ΔX is increment position movement in unit time.

The soft computation that happens in the DSP is presented in Fig. 2. The VSI and motor hardware are also presented in conjunction with it to show the actual signal flow to control the IGBT switches.

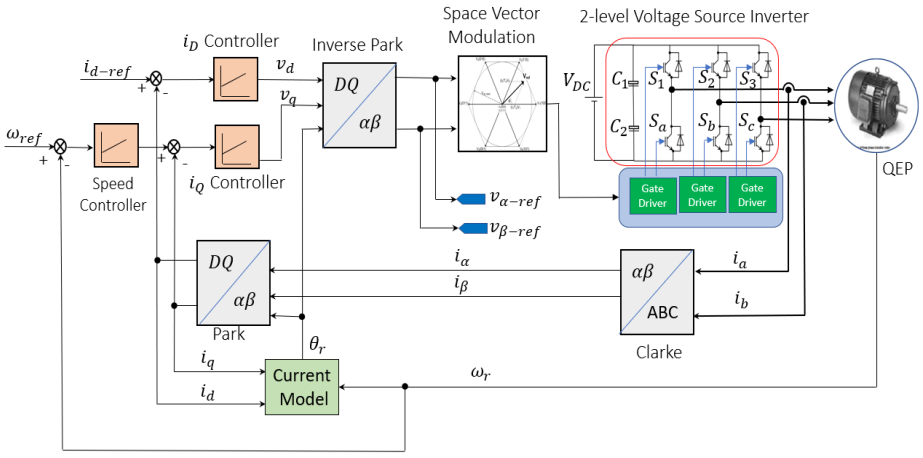

Fig. 2 The proposed vector control algorithm for the speed control of induction motor.

The stator currents of a three-phase alternating electric motor are depicted as two orthogonal components connected by a vector. The third current measurement is not necessary as in the balanced condition $I_a + I_b + I_c = 0$, and thus, two of the phase currents suffice to do the computation. The reference frame transformation from one frame to another is summarized in Fig. 3.

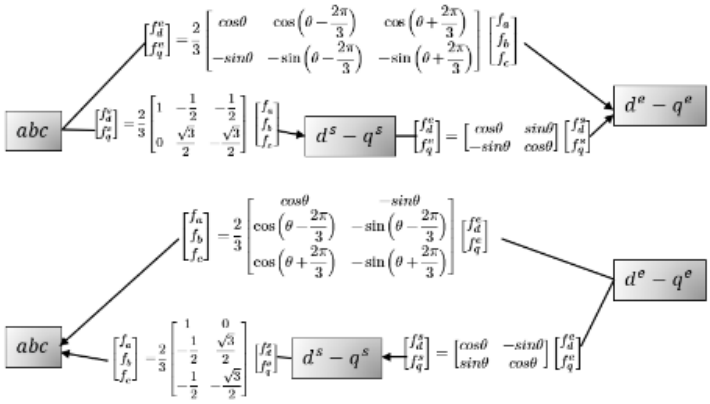

Fig. 1. Reference frame transformation (Summary).

This reference frame transformation can be used for all voltage, current, or flux transformation from 3-phase to 2-phase or vice versa with ease [32].

2.2. Modeling and Simulation of the proposed method

The analysis of the dynamic performance of induction motor has become a priority in addition to steady-state performance analysis to be able to achieve an appropriate control strategy. However, its dynamic stability study is complex because the IM is multivariable, non-linear with an internal coupling effect, and discrete-time in nature. To tackle this problem, the computer simulation study becomes handy particularly when a new control structure is being developed. Once the control structure and parameters of the control system are determined by the simulation study of acceptable performance, a prototype system can be designed and tested with a further iteration of the controller parameters. This requires a mathematical model, which describes the behavior of a motor.

The modeling of induction motor for this study is incorporated from [26]. The modeling and simulation are realized in Matlab/Simulink workbench. The Simulink model for the proposed method is presented in Fig. 4.

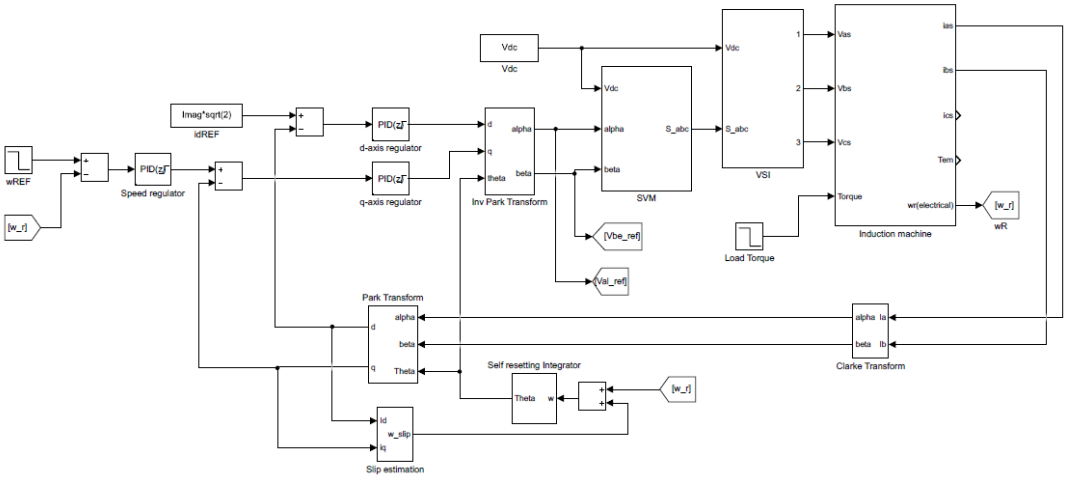

Fig. 4. Simulink model of the proposed method.

The variable-frequency drive's SVM specifies thyristor switching based on the stator voltage references produced by the PI current controllers. The modeling aspect is not included here but extensive details are included in [21, 24, 26]. The controller tuning is performed by adopting the Ziegler-Nichols method.

2.3. Hardware Architecture

The design specification of the general-purpose voltage source inverter for this research is presented in Table 1. Based on the design requirements of the inverter, different component ratings are calculated.

Table 1 General purpose voltage source inverter specification.

Parameter	Specification
Power Rating	70 kVA
Output voltage (max)	400 V
Input voltage (AC)	380 V
Switching Frequency	10 kHz
DC Voltage	600 V
Efficiency	96 %

2.3.1. Rectifier circuit

The fixed AC is converted to variable DC by a diode rectifier. The lightweight, general-purpose, and compact bridge 'Vishay VS-130MT120KPBF' rectifier module is selected for this project. A range of extremely compact, encapsulated three-phase bridge rectifiers offers efficient and reliable operation. They are intended for use in general purposes and heavy-duty applications like an inverter. It can handle 1.2 kV voltage with a maximum DC output current of 130 A.

2.3.2. DC-link capacitor

A DC-link capacitor is fitted in between two converters to provide a low impedance channel for high-frequency switching currents as well as energy storage. It also serves as the power factor correction (PFC) filter; absorbing switching currents to ensure that the ripple voltage is as low as possible [26]. The output stage is a voltage source inverter that takes high-frequency current bursts from the DC-link capacitor. The capacitor must be sized to meet specifications for DC-link ripple voltage and energy storage between mains cycles or when input power is lost. This implies that it should have a low equivalent series resistance (ESR) as well as a low capacitance and ripple current rating. These requirements must be satisfied at the specified operating voltage, temperature, power output, line and switching frequencies, and goal lifespan. The operation of the inverter necessitates pulsed currents from the DC-link side. As a result, DC-link capacitors are necessary to convey these currents while preventing them from reflecting on the source side. The value of the DC-link capacitor can be calculated as

$$C_{dc}=\frac{P_{rated}}{4\times f\times\left(V_{dc}^{2}-\left(V_{dc}-V_{ripple}\right)^{2}\right)} \tag{3}$$

Where, C_{dc} is required minimum capacitance value, P_{rated} is the rating of the converter, V_{dc} is the DC-link voltage, V_{ripple} is the expected ripple voltage, and f is the frequency. The voltage ripple can be obtained by conducting a simple simulation.

Two dc-link capacitors of 2200 μF (400 V) each are connected in series to have a voltage capacity of 800 V. The combination is, in turn, are connected in parallel to the DC busbar.

2.3.3. Inverter

The inverter is a DC-to-AC converter connected to a DC-link capacitor from the DC side and motor to the AC side. It has 6 semiconductor switches connected to a bridge. The switches can be chosen by considering the maximum blocking voltage and the needed current rating. Furthermore, the frequency of switches is determined by the system's intended switching frequency. The IGBT is chosen for this application because of its capability to handle high power and frequency. The three-phase AC voltage is generated by switching these switches simultaneously to synthesize the DC input by generating a gate signal generated from the gate driver. The switches must be controlled in such a way that not both the switches in the same leg turn on or off at the same time to reduce the switching frequency and dead short circuit of the bridge causing damage to an inverter and associated devices [21, 23]. The dead band creates a delay in the complementary switching of two switches in the same leg. Thus, it assures that the magnetic devices don't produce intolerable acoustic noise and exhibit larger control bandwidth [25].

Three numbers of dual half-bridge N-channel 'Semikron SKM100GB12T4' IGBT modules are chosen with a maximum current rating of 160 A and 1.2 kV to suit the design requirement.

Each IGBT bridge has three coupling capacitors (1 μF) attached across it. The gate driver circuit for each leg of the IGBT bridge linked to the heat-sink takes an SVM signal from the DSP in the 0 or 3.3 V range and amplifies it to 0 or 9 V. Apart from its primary purpose of providing the SVM gate pulse to IGBTs, the gate driver also safeguards the inverter. The final product is presented in Fig. 5.

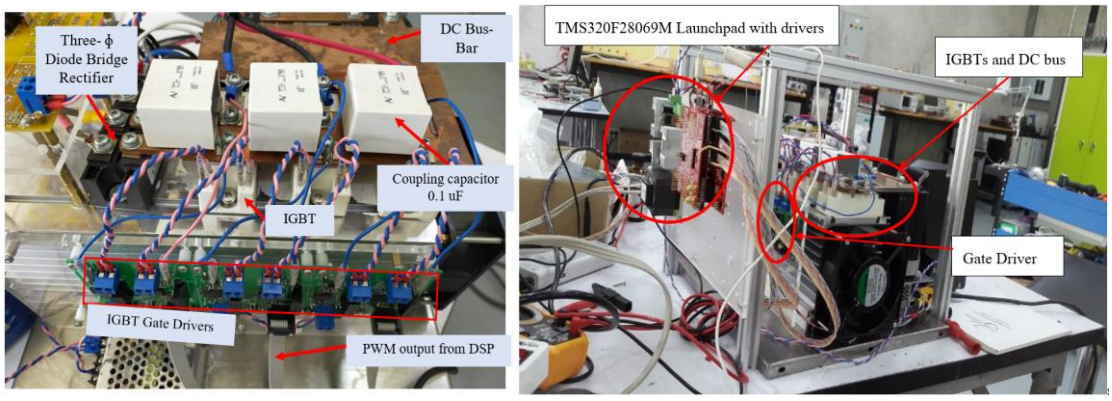

Fig. 5 Laboratory assembled converter: Top view (left), side view (right).

2.3.4 DSP Programming

The DSP program is developed in PC with Code Composer Studio (CCS) IDE installed. The program is deployed to the hardware by USB interface.

To save the cost of implementation, most DSPs are designed to perform arithmetic operations only on integer numbers. An implied binary point is used to represent fractional numbers on these processors. Texas Instrument has improved in their DSP by developing CCS IDE which works best on fractional numbers together with integers by converting to Q-format. It has the fractional bits and integer bits (optional) specified. For example, a Q26 number has 26 fractional bits, and Q1.15 has 1 integer and 15 fractional bits. The program flow while executing follows the flowchart illustrated in Fig. 6.

3. Results and Discussion

The closed-loop control behavior of the 3 HP induction motor whose parameters are specified in Table 2 is presented in this section. The prime objective for performing simulation studies is to closely mimic the actual system. The controller gains are first validated by simulating in software to see the dynamic behavior of the machine according to the reference speed. This is the first step to the development of a hardware system. It is to be noted here that the dynamic study was performed both in simulation and in the hardware to examine with similar set points, thus the difference in time scale doesn't affect the result analysis.

Table 2 Motor Parameters.

Parameters	Specifications
Motor Power	2.2 kW (3 HP)
Voltage	380 V
Current	5 A
frequency	50 Hz
Stator resistance	3.12 Ω
Rotor resistance	3.00 Ω
Stator leakage inductance	12.64 mH
Rotor leakage inductance	12.64 mH
Mutual inductance	301.7 mH
Rotor inertia	0.2 kg.m^2
Rated speed	1420 rpm

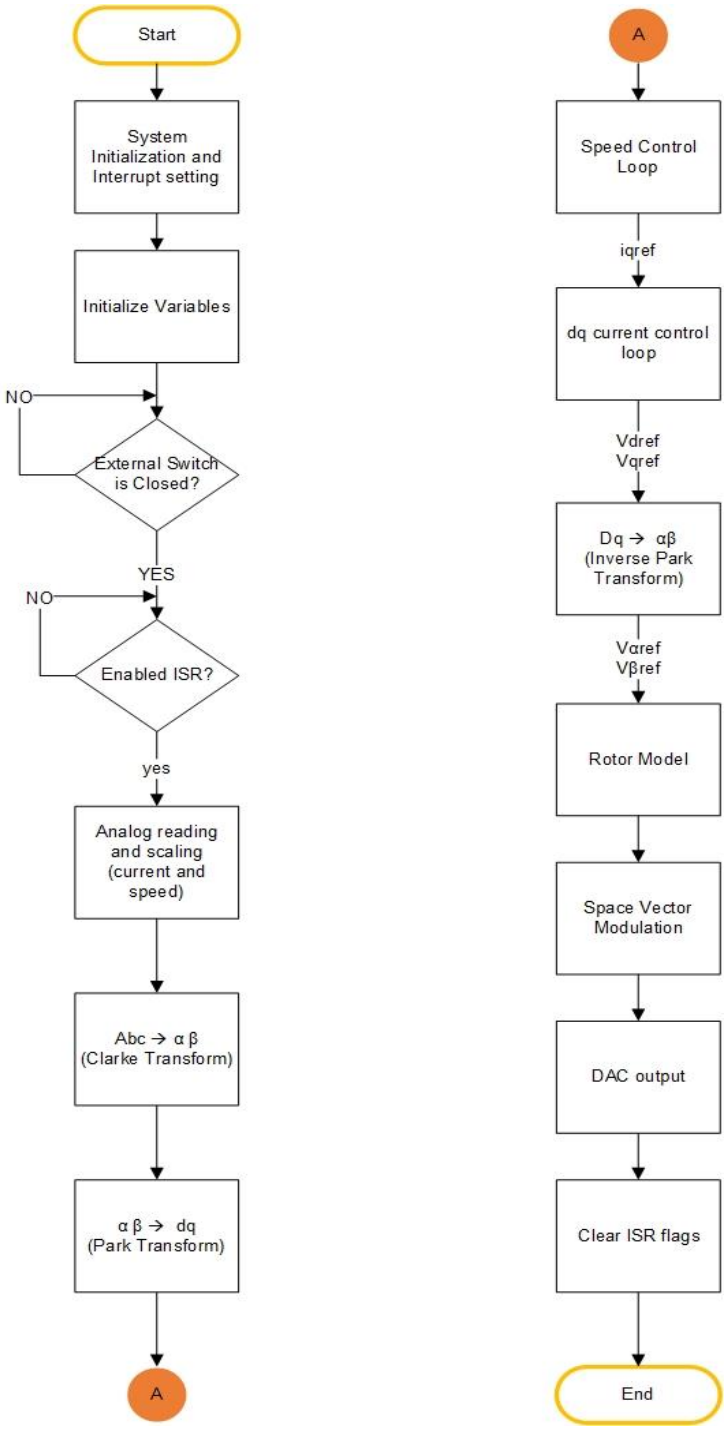

Fig. 6 Control Flow Chart of the program in DSP using CCS.

3.1. Simulation Results

The simulation was performed on the Simulink workbench. Fig. 7 illustrates dynamic behavior exhibited by the motor under different reference speed conditions. As evident from fig. 7 (a), the reference speed is varied randomly from zero to full speed. To study the worst-case scenario, the motor is simulated for zero speed (0 to 0.5 sec) as well as for the 10 % speed (7.7-9.5 sec). Although the

motor is forced to experience different dynamic conditions, the current drawn by the motor is still within the permissible limit compared to twice or thrice the current drawn in traditional starting methods which are evident from fig. 7 (b). The total current harmonics is calculated to be as low as 2.3 much lower than what is expected to be produced by the converter system. The orthogonal $d-q$ currents are also presented in fig. 7 (c) to understand the effectiveness of the controller behavior and observe the control parameters. It is observed that the I_q is saturated at the dynamic instants due to the high requirement of torque than it's rated to meet the demand.

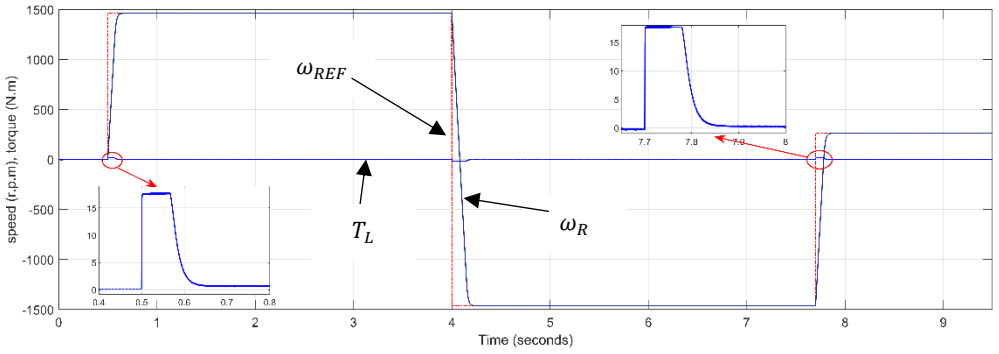

(a)

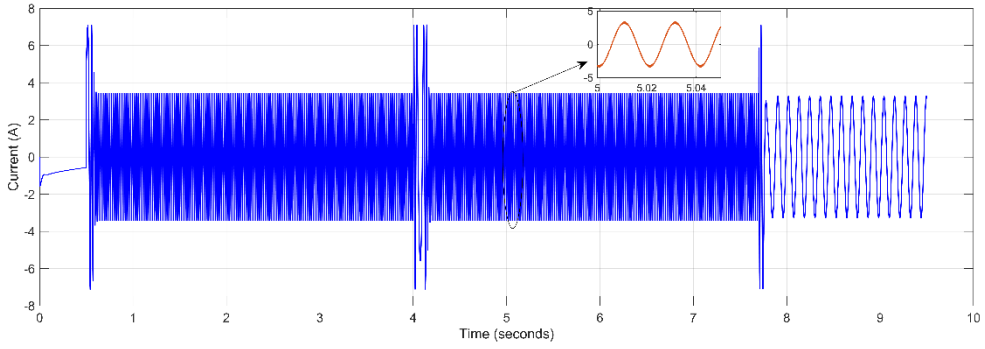

(b)

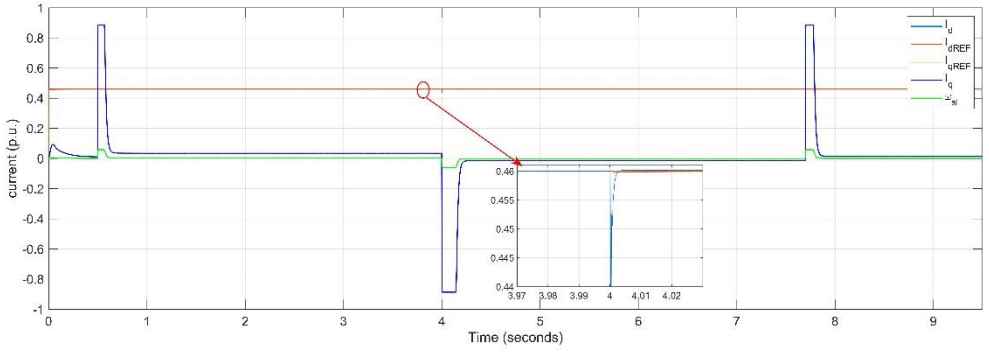

(c)

Fig. 7 Simulation result plotted in MATLAB SIMULINK: (a) speed, (b) line currents, and (c) Torque and i_q and i_d current.

3.2. Laboratory Results

The practical machine behavior is presented in fig. 8. It is evident from fig. 8 (a) that the motor can track the reference value precisely as expected as the simulation results. On the contrary, as evident from fig. 8 (b), the current drawn by a motor during dynamics is twice the actual current drawn at full speed which is higher than that exhibited in the simulation result.

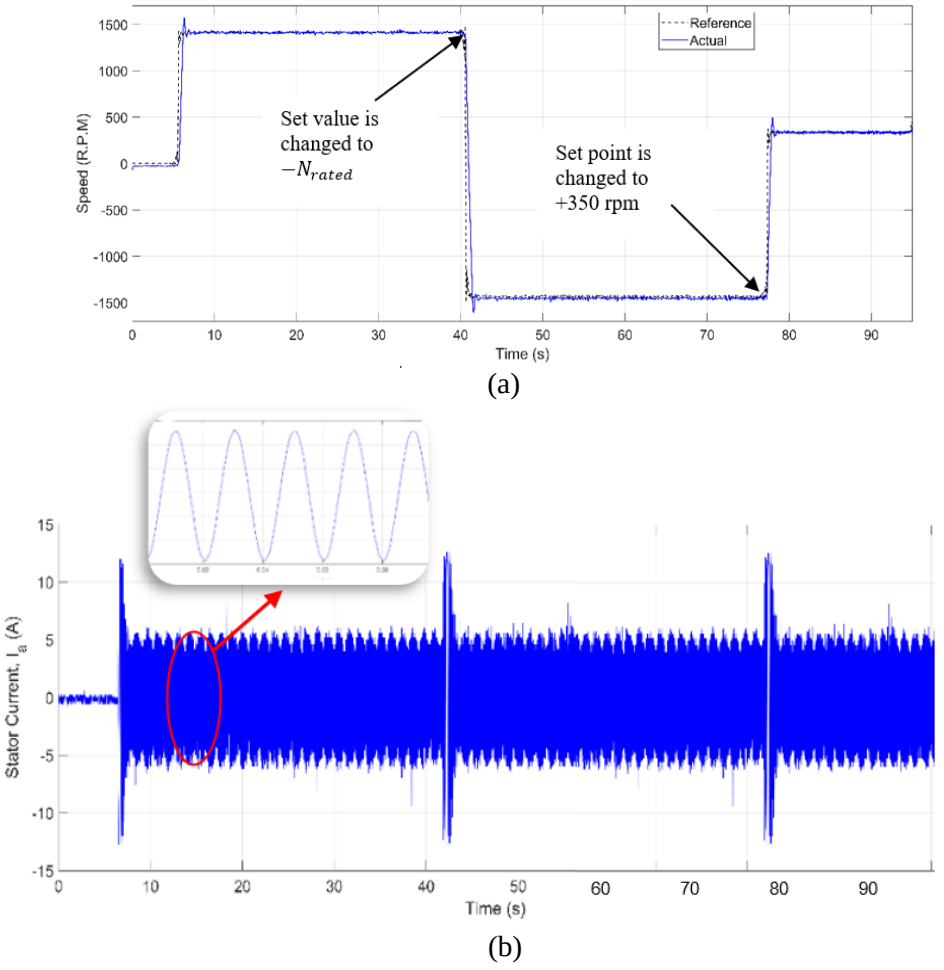

Fig. 8. Practical speed tracking of the motor derived from speed encoder

Moreover, the total current harmonic was 3.65 % which is 1.35 % higher than the simulation results.

3.3. Discussion

The FOC has resulted in almost no torque ripple and very little stator current ripple as evident from the simulation and experimental results. Thus, this algorithm can be adapted to be implemented in wide applications especially in EVs [27]. Moreover, the developed VSI can be used for running two parallel machines due to its ability to provide 12 PWM signals and the design is large enough for this arrangement thus reducing the cost [28]. It is good to note that the inverter can only produce a limited number of discrete voltage vectors. It is because it employs only those fundamental vectors, thus it falls short of meeting control requirements, especially in high transients. The two-vector-based model predictive control and multiple-vector-based model predictive control could be one way to tackle it [29-

30]. Also, the FOC is still difficult to understand, the DTC-SVM has been proposed as the alternative in most of the works of literature [4, 11-12, 19, 31].

4. Conclusion

The result obtained was possible to achieve tighter speed control, higher starting torque, and higher low-speed torque due to the combination of advantages offered by SVM, IFOC, and laboratory-developed converter. As the device is programmed to work with a 20 kHz switching frequency, the inverter was found to be exhibiting larger control bandwidth. Moreover, with a sufficient magnitude of DC-link voltage (600 V) is provided, a fast control loop could be designed which keeps the stator currents close to the set value resulting in a smaller value of current harmonics. Thus, it nullifies the effects of stator voltage on the dynamics of the drive resulting in a considerably simplified and cheap proportional-integral controller. This so happens because the stator voltage interaction is dealt with by the current controllers employing space vector modulation techniques.

Acknowledgements

As this paper is the outcome of the master's thesis, the principal author acknowledges His Majesty's Secretariat (Thimphu), Royal University of Bhutan, and Naresuan University for funding the Masters' study.

References

[1] Nie, Z., Preindl, M., & Schofield, N. (2016, April 19-21). *SVM strategies for multiphase voltage source inverters.* 8th IET International Conference on Power Electronics, Machines and Drives (PEMD 2016), Glasgow.

[2] Bourhichi, S. E., Oukassi, A., Bahir, L. E., & Adnani, M. E. (2021, April 9). *Indirect vector control of induction motor based on five-level inverter cascaded H-Bridge using Space Vector Modulation.* 8th International Conference on Electrical and Electronics Engineering (ICEEE), Antalya.

[3] Zhang, Y., & Bai, Y. (2017, June 3-7). *Model predictive flux control of three-level inverter-fed induction motor drives based on space vector modulation.* IEEE 3rd International Future Energy Electronics Conference and ECCE Asia (IFEEC 2017 - ECCE Asia), Kaohsiung.

[4] Yuan, J., Ma, X., & Liu, J. (2015, May 14-16). *Simulation research of induction motor based on SVM-DTC with a three-level inverter.* IEEE 5th International Conference on Electronics Information and Emergency Communication, Beijing.

[5] Vinod, B. R., Shiny, G., & Baiju, M. R. (2017, July 14-17). *Space vector direct torque control for five-level open-end winding induction motor drive to suppress harmonic spikes.* IEEE Region 10 Symposium (TENSYMP), Cochin.

[6] Jacob, J., Chitra, A., Thomas, R. V., Rakesh, E., Jacob, S., Baby, M., & Cini, K. (2017, February 3-4). *Space vector pulse width modulation for a seven-level inverter applied to an induction motor drive*. International Conference on Innovations in Electrical, Electronics, Instrumentation and Media Technology (ICEEIMT), Coimbatore.

[7] Tang, Q., Ge, X., & Liu, Y.-C. (2016, May 22-26). *Performance analysis of two different SVM-based field-oriented control schemes for eight-switch three-phase inverter-fed induction motor drives*. IEEE 8th International Power Electronics and Motion Control Conference (IPEMC-ECCE Asia), Hefei.

[8] Sakti, P. S. B., & Riyadi, S. (2019, September 21-22). *Hardware implementation of simplified VVVF inverter for induction motor based on SVM.* 2019 International Seminar on Application for Technology of Information and Communication (iSemantic), Semarang.

[9] Das, B. (2016). Vector control of 3-phase induction motor by Space Vector Modulation. *International Journal of Engineering Science and Computing*, *6*(7), 8587–8591.

[10] Banerjee, T., Bera, J. N., Chowdhuri, S., & Sarkar, G. (2016, January 28-30). *A comparative study between different modulations techniques used in field oriented control induction motor drive*. 2016 2nd International Conference on Control, Instrumentation, Energy Communication (CIEC), Kolkata.

[11] Malla, S. G. (2016, March 3-5). *A review on Direct Torque Control (DTC) of induction motor: with applications of fuzzy.* 2016 International Conference on Electrical, Electronics, and Optimization Techniques (ICEEOT), Chennai.

[12] Kale, S. S., & Pawaskar, R. C. (2018, February 8-9). *Analysis of torque and flux ripple factor for DTC and SVM - DTC of induction motor drive.* 2018 International Conference On Advances in Communication and Computing Technology (ICACCT), Ahmednagar.

[13] A. S. Muktar, T., R. Umale, A., & K. Kirpane, R. (2017). Vector control methods for variable speed of AC motors. *International Research Journal of Engineering and Technology (IRJET)*, *4*(2), 340–343.

[14] Parthan, A., Suresh, L. P., & Raj, J. R. A. (2017, April 20-21). *A brief review on torque control of induction motor*. 2017 International Conference on Circuit, Power and Computing Technologies (ICCPCT), Kollam.

[15] Ammar, A., Bourek, A., Benakcha, A., & Ameid, T. (2017, May 7-9). *Sensorless stator field oriented-direct torque control with SVM for induction motor based on MRAS and fuzzy logic regulation.* 2017 6th International Conference on Systems and Control (ICSC), Batna.

[16] Wu, X., Huang, W., & Lin, X. (2019, August 11-14). *A novel direct torque control with or without duty ratio optimization for induction motors*. 2019 22nd International Conference on Electrical Machines and Systems (ICEMS), Harbin.

[17] User, Y., & Tabanli, N. (2017, October 11-13). *Development of induction motor torque control algorithm for electric vehicles on inclined roads.* 2017 International Conference on Electromechanical and Power Systems (SIELMEN), Iasi.

[18] Mahanta, U., Patnaik, D., Panigrahi, B. P., & Panda, A. K. (2015, June 12-13). *Dynamic modeling and simulation of SVM-DTC of five-phase induction motor.* 2015 International Conference on Energy, Power and Environment: Towards Sustainable Growth (ICEPE), Shillong.

[19] Sahu, A., Mohanty, K. B., & Mishra, R. N. (2021, January 2-3). *Design of MPC-PSO-based torque regulator for DTC-SVM induction motor drive.* 2021 1st International Conference on Power Electronics and Energy (ICPEE), Bhubaneswar.

[20] Alsofyani, I. M., & Idris, N. R. N. (2016). Simple Flux Regulation for Improving State Estimation at Very Low and Zero Speed of a Speed Sensorless Direct Torque Control of an Induction Motor. *IEEE Transactions on Power Electronics*, *31*(4), 3027–3035.

[21] Karchung, & Ruangsinchaiwanich. S. (2019). Open-loop vector control of induction motor with space vector pulse width modulation technique. *International Journal of Electrical and Computer Engineering*, *13*(9), 6.

[22] Mirzaei, M., & Dastfan, A. (2019, February 12-14). *A novel space vector modulation strategy for direct torque control of induction motors.* 2019 10th International Power Electronics, Drive Systems and Technologies Conference (PEDSTC), Shiraz.

[23] Karchung, K., & Ruangsinchaiwanich, S. (2019, November 23-25). *Performance evaluation of sensorless vector controlled induction motor with fuzzy-based rotor-flux MRAS.* 2019 2nd International Conference on Computational Intelligence and Intelligent Systems, Bangkok.

[24] Divyasree, P., & Binojkumar, A. C. (2017, August 1-2). *Vector control of voltage source inverter fed induction motor drive using space vector PWM technique.* 2017 International Conference on Energy, Communication, Data Analytics and Soft Computing (ICECDS), Chennai.

[25] Leonhard, W. (2001). *Control of electrical drives* (3rd ed.). Berlin, Germany: Springer Berlin, Heidelberg.

[26] Karchung, K. (2020). *Sensorless field oriented control of three-phase induction motor using fuzzy PI controller* (Master's thesis). Phitsanulok, Naresuan University.

[27] BV, P., Balamurugan, A., Selvathai, T., Reginald, R., & Varadhan, J. (2019, August 21-23). *Evaluation of different vector control methods for electric vehicle application.* 2019 2nd International Conference on Power and Embedded Drive Control (ICPEDC), Chennai.

[28] Afje, M. G. (2015, November 23-25). *Dynamic performance of single inverter fed parallel induction motors.* 2015 30th International Power System Conference (PSC), Tehran.

[29] Zhang, Y., Bai, Y., & Yang, H. (2018). A universal multiple-vector-based model predictive control of induction motor drives. *IEEE Transactions on Power Electronics, 33*(8), 6957–6969.

[30] Zhang, Y., & Bai, Y. (2017, August 11-14). *An efficient two-vector-based model predictive control for induction motor drives.* 2017 20th International Conference on Electrical Machines and Systems (ICEMS), Sydney.

[31] Listwan, J., & Pienkowski, K. (2018, June 10-13). *Experimental studies of DTC-SVM control of six-phase induction motor with application of the super-twisting sliding mode controllers.* 2018 International Symposium on Electrical Machines (SME), Andrychow.

[32] Kim, S. H. (2017). *Electric Motor Control: DC, AC, and BLDC Motors* (1st ed.). Massachusetts, USA: Elsevier Science.